LETTER

Improving robustness of spatial networks via reinforced nodes

To cite this article: Nir Vaturi *et al* 2023 *EPL* **142** 61002

A LETTERS JOURNAL EXPLORING
THE FRONTIERS OF PHYSICS

June 2023

EPL, **142** (2023) 61002
doi: 10.1209/0295-5075/acd9e9

www.epljournal.org

Improving robustness of spatial networks via reinforced nodes

NIR VATURI[(a)], BNAYA GROSS[(b)] and SHLOMO HAVLIN

Department of Physics, Bar-Ilan University - Ramat-Gan 52900, Israel

received 8 March 2023; accepted in final form 30 May 2023
published online 12 June 2023

Abstract – Many real-world networks are embedded in space, and their resilience in the presence of reinforced nodes has not been studied. In this paper, we use a spatial network model with an exponential distribution of link length r and a characteristic length ζ to model such networks. We find that reinforced nodes can significantly increase the resilience of the networks, which varies with the strength of spatial embedding. We also study different reinforced node distribution strategies for improving the network's resilience. Interestingly, we find that the best strategy is highly dependent on the expected magnitude of failures which we analyze using percolation theory. Finally, we show that the reinforced nodes are analogous to an external field in the percolation phase transition and that their critical exponents satisfy Widom's relation.

Introduction. – Network theory has made a significant contribution to understanding the complexity of different systems, such as communication networks [1], transportation systems [2] and even neuronal networks [3, 4]. The resilience of such networks is often studied under a percolation process [5–8] where a fraction $1-p$ of nodes is removed from the network (*i.e.*, removed from the system along with their edges) and the size of the largest connected component, P_∞ is evaluated. It has been found that these networks experience a second-order phase transition at a critical point p_c [9]. For infinitely large networks, the size of the giant component below the transition point is zero, while it is non-zero above it. The giant component is used to describe the network functionality, where nodes that are connected to it are considered functional, while isolated clusters are considered non-functional.

Many real-world networks are spatially embedded [10–15], and it has been shown that the spatiality of a network affects the phase transition of the percolation process [16]. Examples of such spatial networks are infrastructure networks [17], brain network [10], and transportation networks [18–20]. Percolation processes have been thoroughly studied for complex networks [9,21–23] also for evolution and cooperation dynamics [24–26], but the robustness of spatial networks in the presence of reinforced nodes has not been studied.

Recently, the question of centralization *vs.* decentralization of infrastructures has emerged, which led to the idea of reinforced nodes. These reinforced nodes can function and support other nodes in their cluster even if they are not connected to the giant component [27,28] and can be significant for the robustness of real-world networks. For example, in the case of the internet, satellites [29] can also be used in order to exchange information, meaning they are functional without being directly connected to the giant component. Another example are power grids, where reinforced nodes represent generators, each having their own source of energy and being able to support themselves and their clusters. The importance of reinforced nodes goes beyond pairwise interaction networks and is valid also for real-world networks with high-order interactions [30] and may also have applications for living systems [31]. In this paper, we will study the effects of reinforced nodes on spatial networks and analyze different approaches to distributing them.

Model. – Our model is composed of a $2D$ square lattice of size $N = L \times L$, with bi-periodic boundary conditions, that is initially devoid of links. Following that, we add links with length r at random from an exponential decaying distribution [14,16,32–34],

$$P(r) \sim e^{-r/\zeta}, \tag{1}$$

where ζ is the characteristic length of the links. In this model, long-range links are rare due to the decay of the distribution, which represents the realistic constraint of the high cost of long-range links [35].

The process of creating a spatial network requires 3 successive steps. The first step is to randomly choose a node. The second step is to randomly draw a link length from

(a) E-mail: Nir315@gmail.com
(b) E-mail: bnaya.gross@gmail.com (corresponding author)

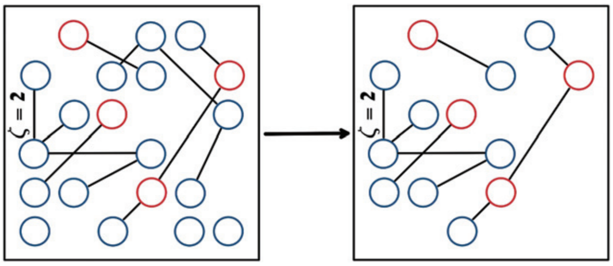

Fig. 1: Illustration. The nodes are placed as the sites of a $2D$ square lattice with bi-periodic boundary conditions, while the links are added according to eq. (1). The characteristic length of the links is ζ (left link in both boxes), while a small fraction ρ of the nodes are randomly reinforced (red nodes). Left: the network, at a certain point in the percolation process, contains the giant component and finite clusters. Right: P_∞ represents the functioning nodes in the network, *i.e.*, it includes all nodes that are part of the giant component or connected to a finite cluster with at least one reinforced node, a total of 13 nodes.

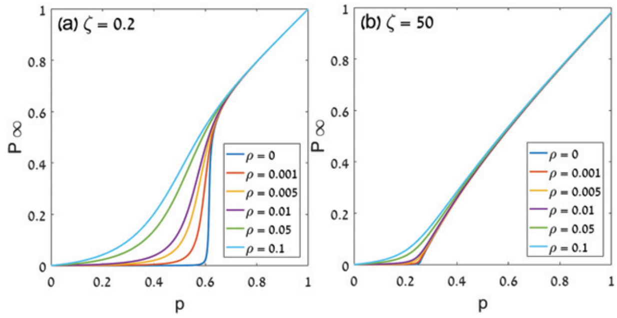

Fig. 2: Randomly distributed reinforced nodes in spatial networks. (a) The giant component, P_∞, as a function of p for $\zeta = 0.2$ (similar to $2D$ lattice). The phase transition at $p_c \simeq 0.59$ is being removed by even a small fraction of reinforced nodes. The network becomes more resilient as the fraction of reinforced nodes increases. (b) The giant component, P_∞, as a function of p for $\zeta = 50$. As ζ increases, we can see similar results but a significantly weaker effect compared to (a). Note, due to large ζ, the phase transition is close to the ER limit of $p_c = 0.25$. Here $\langle k\rangle = 4$ and $N = 10^6$.

the distribution in eq. (1). The third step is to randomly choose an angle, identify the closest target node for the link, and create an edge. For our specific model, we chose the average degree (number of links) of the nodes to be $\langle k\rangle = 4$. In order to achieve a given $\langle k\rangle$ we repeat these steps $N \cdot \langle k\rangle/2$ times.

It is important to note that for $\zeta \to 0$ our model generates a $2D$ lattice, where each node is connected only to its nearest neighbors and has a known value of $p_c \simeq 0.59$ [13]. On the other hand, for $\zeta \to \infty$ our model generates an ER network, where all links have a pre-determent probability of being cast, and has a known value of $p_c = 1/\langle k\rangle$ [13].

After generating the spatial network, we chose a fraction ρ of nodes to be reinforced nodes (see fig. 1). The reinforced nodes are chosen randomly, with the only condition being that the nodes are part of the original giant component of the network. We now use the notation P_∞ as the fraction of *functioning* nodes in the network and we analyze P_∞ as a function of p, where $1-p$ is the fraction of removed nodes along with their edges.

Results. – The resilience of spatial networks can be studied using percolation process for the model above where reinforced nodes are randomly distributed and support their clusters. Figure 2 shows the results for different values of ζ and different values of ρ. We included only 2 values of ζ in the figure, other values of ζ show similar results and can be seen in the Supplementary Material `Supplementarymaterial.pdf` (SM). As can be seen, the existence of reinforced nodes, which can function and support other nodes in their cluster even if they are not connected to the giant component, makes the spatial network more resilient to random failures. Since a fraction of $1-p$ of nodes are randomly removed from the networks, a fraction of $p \cdot \rho$ of the reinforced nodes remains active on average. Thus, only for $p = 0$ the giant component will be zero and therefore the percolation transition is removed. It can also be seen that the higher the fraction of reinforced nodes, the more resilient the network. And lastly, as the network is more spatial, *i.e.*, the lower the ζ, the higher is the impact of the reinforced nodes on the network.

Once we establish that reinforced nodes significantly increase the resilience of spatial networks, we can address the question of identifying better strategies, *i.e.*, we can ask what the best strategy to distribute the reinforced nodes to maximize the network's resilience is. To do so, we repeated the percolation process for different values of ζ and ρ testing 6 different distribution strategies:

- Random distribution, as shown in fig. 2.
- Nodes with the highest degree k.
- Nodes with the lowest degree k.
- Nodes with the longest average link length.
- Nodes with the shortest average link length.
- Nodes with the highest weighted degree, defined as

$$w_i = \sum_{j=1}^{N} A_{ij}\sqrt{(x_i - x_j)^2 + (y_i - y_j)^2}, \qquad (2)$$

where A_{ij} is the adjacency matrix and (x_i, y_i) is the geometric location of node i. The weighted degree strategy is a combination of the four previous strategies since it takes into consideration both the average length of the links and the degree k of the node.

As we can see in fig. 3(a)–(c), the functionality of the network changes depending on the distribution strategy of the reinforced nodes. For high values of p, the best distribution strategy for reinforced nodes is low-degree nodes.

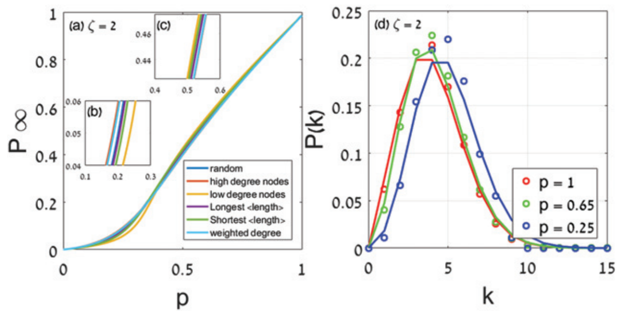

Fig. 3: Strategies for reinforced nodes distribution. (a) P_∞ as a function of p for 6 different strategies of reinforced nodes distribution: random distribution, high-degree and low-degree node preference, longest and shortest average length preference, and weighted degree preference. Here $\zeta = 2$. (b) Zoom in of the lower values p (below p_c). The best nodes to reinforce are the nodes with the highest degree, and the worst nodes to reinforce are the nodes with the lowest degree. (c) Zoom in for the high values p (above p_c). The best strategies are reversed compared to (b). Here $\rho = 0.1$. (d) The degree distribution of the nodes having degree k in the giant component. Here $\zeta = 2$ and $\rho = 0$. As can be seen, the distribution shifts to the right for low values of p, *i.e.*, towards larger degree values. Thus, for high values of p, it is more useful to reinforce low-degree nodes since they fail more frequently, while at low values of p it is better to reinforce high-degree nodes. We can see that our simulation results (circles) and the analytic MF solution (continuous line, see the SM) are in good agreement, indicating that although the analytical solution is based on MF theory, it also catches quite well the behavior of spatial networks. Here $\langle k \rangle = 4$ and $N = 10^6$.

In contrast, for low values of p, the best distribution strategy is to reinforce high-degree nodes. These results are shown for $\zeta = 2$, but are valid also for other values of ζ (see the SM). In order to understand why the percolation process has different best distribution strategies for reinforced nodes for different values of p, we study the distribution of the degree k of nodes in the giant component for different values of p. We find, as shown in fig. 3(d), that the distribution is shifting for lower values of p towards large degrees, which means that where failures are small (*i.e.*, large p), low-degree nodes have a much higher probability to be disconnected from the giant component. In this case, making low-degree nodes reinforced improves the robustness, while for large damage (low values of p below p_c), high-degree nodes start to disconnect from the giant and are therefore preferred to be chosen as reinforced nodes. Another way to understand this phenomenon is that high-degree nodes are associated with larger finite clusters. However, when p is high, most of the high-degree nodes are still part of the giant component and therefore reinforcing them does not contribute to the robustness. In contrast, when p is low, there are many high-degree nodes that have been disconnected, and reinforcing them increases the robustness.

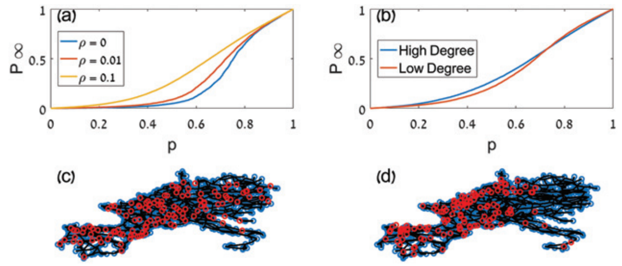

Fig. 4: Impact of reinforced nodes on the power grid network of Europe. (a) Randomly distributed reinforced nodes in the power grid network of Europe [16]. The higher the fraction of reinforced nodes, the more resilient the network becomes, similar to our model. (b) High- and low-degree reinforced distribution strategies. Similar to fig. 3, the best strategy is dependent on the magnitude of random failures. (c) An illustration of the EU power grid network with reinforced nodes on the nodes with the highest degrees k. (d) An illustration of the EU power grid network with reinforced nodes on the nodes with the lowest degrees k. For both (c) and (d), the blue circles represent the regular nodes, the red circles represent the reinforced nodes, and the black lines are the links between the nodes in the network. For panels (b)–(d) $\rho = 0.1$.

Test on a real network: the EU power grid. – To further validate our results, we studied the impact of reinforced nodes on the EU power grid network. The edge distribution of this network was found to follow eq. (1) [16]. The number of nodes in the network is $N = 1254$, while the average degree is $\langle k \rangle = 1.44$ [16]. The system size here is much smaller compared to our simulations before. Thus, we expect the results to be noisy and, due to the lower average degree $\langle k \rangle$, have a higher value of p_c.

In fig. 4(a) we demonstrate the impact of randomly distributed reinforced nodes in a real-world network, the EU power grid, for different values of ρ. As one can see, we get similar results to those found in our model. As shown in fig. 2, the presence of a small fraction of reinforced nodes makes the network significantly more resilient. In fig. 4(b) we show the percolation process of the power grid of Europe network with 2 strategies according to fig. 3, low-degree distribution and high-degree distribution. We can clearly see similar results to our model. For low-damage from the percolation process, it is better to reinforce the nodes with a lower degree, while for high-damage from the percolation process, it is better to reinforce the nodes with a higher degree. In fig. 4(c), (d) we can see the power grid network of Europe with low-degree and high-degree distribution strategies.

External field analogy. – Here we argue that the concentration ρ of reinforced nodes is analogous to external field in percolation [6,8]. The key critical exponents β, δ, and γ that describe the behavior of the system near criticality will be derived below [32,36]. These key critical exponents also satisfy Widom's identity $\delta - 1 = \gamma/\beta$ [6,8,27,36,37].

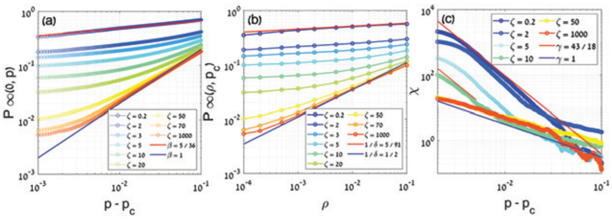

Fig. 5: Critical exponents and external field analogy. (a) The critical exponent β. A crossover is observed from the two limits of $\beta_{2D} = 5/36$ and $\beta_{MF} = 1$ as ζ varies. (b) The critical exponent δ. Similar to β, there is a crossover between $\delta_{2D} = 91/5$ and $\delta_{MF} = 2$. (c) The critical exponent γ. Also here there is a crossover between $\gamma_{2D} = 43/18$ and $\gamma_{MF} = 1$. Here $\langle k \rangle = 4$ and $N = 10^7$.

The critical exponent β describes the behavior of the order parameter P_∞ near the critical point with zero-field ($\rho = 0$, *i.e.*, no reinforced nodes) and is given by

$$P_\infty(0, p) \sim (p - p_c)^\beta \,. \tag{3}$$

At the critical point, ($p = p_c$), the increase of the order parameter with the magnitude of the field, *i.e.*, the concentration of reinforced nodes ρ, is expected to yield the critical exponent δ as

$$P_\infty(\rho, p_c) \sim \rho^{1/\delta}. \tag{4}$$

The susceptibility of the system, χ, is given by the partial derivative of the order parameter with respect to the field, ρ, and scales near the critical point with the exponent γ as

$$\chi \equiv \left(\frac{\partial P_\infty(\rho, p)}{\partial \rho} \right)_{\rho \to 0} \sim |p - p_c|^{-\gamma}. \tag{5}$$

As shown in fig. 5, all critical exponents show a crossover between their known values for the $2D$ lattice and the ER network as ζ changes [32]. For strong spatiality (*i.e.*, low values of ζ), we obtain $\beta = 5/36$, $\delta = 91/5$, and $\gamma = 43/18$, while for weak spatiality (*i.e.*, high values of ζ), we find $\beta = 1$, $\delta = 2$, and $\gamma = 1$, which are the known values for these critical exponents for both of these networks. Both sets of critical exponents satisfy Widom's identity $\delta - 1 = \gamma/\beta$ [6,8]. This crossover is a result of different behaviors on different scales. In short scales below ζ all nodes can connect with the same probability similar to ER networks and thus the MF exponents are valid. However, above ζ a spatial behaviour is observed and $2D$ critical exponents are observed [32].

Summary. – We showed that reinforced nodes have a significant effect on the resilience of spatial networks. Even a small fraction of reinforced nodes remove the percolation phase transitions and increase the functional component. We showed that the higher the fraction of reinforced nodes, the more resilient the network, *i.e.*, the functional component increases. We also found that the lower the value of ζ, the stronger the effect of the same fraction of reinforced nodes on the resilience of the network. We showed that the best reinforced node distribution strategy highly depends on the magnitude of the random failures. For low damage from the percolation process, low $1 - p$, it is better to reinforce the low-degree nodes, while for high damage from the percolation process, it is better to reinforce the high-degree nodes. We also showed the effect of reinforced nodes in a real-world spatial embedded network. Finally, we showed that reinforced nodes are analogous to external field also in the presence of spatial constraints with a crossover phenomenon for intermediate values of ζ and that the critical exponents that we found satisfy Widom's identity $\delta - 1 = \gamma/\beta$.

* * *

We thank the Israel Science Foundation, the Binational Israel-China Science Foundation Grant No. 3132/19, ONR, NSF-BSF Grant No. 2019740, the EU H2020 project RISE (Project No. 821115), the EU H2020 DIT4TRAM, the EU Horizon grant OMINO (No. 101086321) and DTRA Grant No. HDTRA-1-19-1-0016 for financial support. BG acknowledges the support of the Mordecai and Monique Katz Graduate Fellowship Program.

Data availability statement: No new data were created or analysed in this study.

REFERENCES

[1] Lambiotte Renaud, Blondel Vincent D., De Kerchove Cristobald, Huens Etienne, Prieur Christophe, Smoreda Zbigniew and Van Dooren Paul, *Phys. A: Stat. Mech. Appl.*, **387** (2008) 5317.

[2] Zeng Guanwen, Li Daqing, Guo Shengmin, Gao Liang, Gao Ziyou, Stanley H. Eugene and Havlin Shlomo, *Proc. Natl. Acad. Sci. U.S.A.*, **116** (2019) 23.

[3] Fornito Alex, Zalesky Andrew and Bullmore Edward, *Fundamentals of Brain Network Analysis* (Academic Press) 2016.

[4] Breakspear Michael, *Nat. Neurosci.*, **20** (2017) 340.

[5] Essam John W., *Rep. Prog. Phys.*, **43** (1980) 833.

[6] Stauffer Dietrich and Aharony Ammon, *Introduction to Percolation Theory* (Taylor & Francis) 2018.

[7] Kirkpatrick Scott, *Rev. Mod. Phys.*, **45** (1973) 574.

[8] Bunde Armin and Havlin Shlomo, *Fractals and Disordered Systems* (Springer Science & Business Media) 2012.

[9] Cohen Reuven, Erez Keren, Ben-Avraham Daniel and Havlin Shlomo, *Phys. Rev. Lett.*, **85** (2000) 4626.

[10] Barthélemy Marc, *Phys. Rep.*, **499** (2011) 1.

[11] Watts Duncan J. and Strogatz Steven H., *Nature*, **393** (1998) 440.

[12] Penrose Mathew, *Random Geometric Graphs*, Vol. **5** (Oxford University Press, Oxford) 2003.

[13] Gross Bnaya and Havlin Shlomo, *Percolation in spatial networks: Spatial network models beyond nearest neighbours structures, Elements in Structure and Dynamics of Complex Networks* (Cambridge University Press) 2022.

[14] Gross Bnaya, Vaknin Dana, Danziger Michael M. and Havlin Shlomo, *Multi-universality and localized attacks in spatially embedded networks*, in *Proceedings of the Asia-Pacific Econophysics Conference 2016, Big Data Analysis and Modeling toward Super Smart Society (APEC-SSS2016)* (JPS) 2017, p. 011002.

[15] McAndrew Thomas C., Danforth Christopher M. and Bagrow James P., *Phys. Rev. E*, **91** (2015) 042813.

[16] Danziger Michael M., Shekhtman Louis M., Berezin Yehiel and Havlin Shlomo, *EPL*, **115** (2016) 36002.

[17] Hines Paul, Blumsack Seth, Cotilla Sanchez E. and Barrows Clayton, *The topological and electrical structure of power grids*, in *2010 43rd Hawaii International Conference on System Sciences* (IEEE) 2010, pp. 1–10.

[18] Strano Emanuele, Giometto Andrea, Shai Saray, Bertuzzo Enrico, Mucha Peter J. and Rinaldo Andrea, *R. Soc. Open Sci.*, **4** (2017) 170590.

[19] Weiss D. J., Nelson Andy, Gibson H. S., Temperley W., Peedell Stephen, Lieber A., Hancher M., Poyart Eduardo, Belchior Simão, Fullman Nancy *et al.*, *Nature*, **553** (2018) 333.

[20] Li Daqing, Fu Bowen, Wang Yunpeng, Lu Guangquan, Berezin Yehiel, Stanley H. Eugene and Havlin Shlomo, *Proc. Natl. Acad. Sci. U.S.A.*, **112** (2015) 669.

[21] Dorogovtsev Sergey N., Goltsev Alexander V. and Mendes José F. F., *Rev. Mod. Phys.*, **80** (2008) 1275.

[22] Cohen Reuven and Havlin Shlomo, *Percolation in complex networks, Complex Media and Percolation Theory* (Springer Verlag) 2021, pp. 419–431.

[23] Callaway Duncan S., Newman Mark E. J., Strogatz Steven H. and Watts Duncan J., *Phys. Rev. Lett.*, **85** (2000) 5468.

[24] Perc Matjaž, *New J. Phys.*, **11** (2009) 033027.

[25] Yang Han-Xin, Rong Zhihai and Wang Wen-Xu, *New J. Phys.*, **16** (2014) 013010.

[26] Wang Zhen, Szolnoki Attila and Perc Matjaž, *Sci. Rep.*, **2** (2012) 369.

[27] Yuan Xin, Hu Yanqing, Stanley H. Eugene and Havlin Shlomo, *Proc. Natl. Acad. Sci. U.S.A.*, **114** (2017) 3311.

[28] Kfir-Cohen Yael, Vaknin Ben Porath Dana and Havlin Shlomo, *EPL*, **137** (2022) 41003.

[29] Henderson Thomas R. and Katz Randy H., *IEEE J. Sel. Areas Commun.*, **17** (1999) 326.

[30] Majhi Soumen, Perc Matjaž and Ghosh Dibakar, *J. R. Soc. Interface*, **19** (2022) 20220043.

[31] Gosak Marko, Milojević Marko, Duh Maja, Skok Kristijan and Perc Matjaž, *Phys. Life Rev.*, **41** (2022) 1.

[32] Bonamassa Ivan, Gross Bnaya, Danziger Michael M. and Havlin Shlomo, *Phys. Rev. Lett.*, **123** (2019) 088301.

[33] Gross Bnaya, Bonamassa Ivan and Havlin Shlomo, *Phys. A: Stat. Mech. Appl.*, **567** (2021) 125644.

[34] Gotesdyner Ouriel, Gross Bnaya, Vaknin Ben Porath Dana and Havlin Shlomo, *J. Phys. A: Math. Theor.*, **55** (2022) 254003.

[35] Gastner Michael T. and Newman Mark E. J., *Eur. Phys. J. B*, **49** (2006) 247.

[36] Fan Jingfang, Dong Gaogao, Shekhtman Louis M., Zhou Dong, Meng Jun, Chen Xiaosong and Havlin Shlomo, *New J. Phys.*, **20** (2018) 093003.

[37] Gross Bnaya, Sanhedrai Hillel, Shekhtman Louis and Havlin Shlomo, *Phys. Rev. E*, **101** (2020) 022316.